Effects of Electrode Properties of a Short Pulse Laser-Assisted Pulsed Plasma

IEPC-2015-456p／ISTS-2015-b-456p

Presented at Joint Conference of 30th International Symposium on Space Technology and Science 34th International Electric Propulsion Conference and 6th Nano-satellite Symposium, Hyogo-Kobe, Japan July 4 – 10, 2015

By Haruna HASEGAWA[1)], Kouta MATSUBARA[2)], Hiroshi HOSOKAWA[2)], Nao AKASHI[2)], Yuji OIGAWA[2)], Hideyuki HORISAWA[3)]

[1)] *Undergraduate student, Department of Aeronautics and Astronautics, Tokai University, Hiratsuka, Kanagawa, 259-1292, Japan*

[2)] *Graduate student, Department of Aeronautics and Astronautics, Tokai University, Hiratsuka, Kanagawa, 259-1292, Japan*

[3)] *Professor, Department of Aeronautics and Astronautics, Tokai University, Hiratsuka, Kanagawa, 259-1292, Japan*

Abstract: In this study, effects of electrode lengths and materials on thrust performance of a short-pulse rectangular laser-assisted pulsed plasma thruster (LAPPT) were investigated. Thrust performance was also examined for various cases with a target pendulum thrust stand in a vacuum chamber. To compare the effects of length and material of the electrodes, electrodes of 5 mm in length and those made of copper were also examined. Moreover, to observe the plasma behavior and the plasma acceleration process, an observation of plasma plume between the rectangular electrodes of the short-pulse laser-assisted pulsed plasma thruster with an ICCD camera was conducted. From the results, impulse bits increased with charge energies for both electrode lengths. Moreover, for shorter electrode length case, it was shown that impulse bits were larger than longer cases. From the results of time-resolved images with the ICCD camera, the plasma emission can only be seen in a limited region of on and near the propellant surface.

Nomenclature

C	=	Capacitance
E_c	=	Charge Energy
V_c	=	Charge Voltage
h	=	Electrode heigh
l	=	Electrode length
w	=	Electrode width
L_E	=	Laser energy
I_{sp}	=	Specific impulse

I. Introduction

THE current trend towards small spacecraft, which is not only mass limited but also power limited, has produced a strong interest in development of micropropulsion devices.[1-4] The significance in reducing launch masses has attracted growing interests in regard to a decrease in mission cost and an increase in launch rate. Although, in the past, many very small spacecraft lacked propulsion systems, future micro-spacecraft will require significant propulsion capability to provide a high degree of maneuverability and capability. The benefit of using electric propulsion for the reduction of spacecraft mass will likely be even more significant for mass limited micro-spacecraft missions.[2-4] Feasibility studies of micro-spacecraft are currently under development for a mass less than 100 kg with an available power level for propulsion of less than 100 watts.[1-4)] Various potential propulsion systems for micro-spacecraft applications, such as ion thrusters, field emission thrusters, pulsed plasma thrusters (PPTs), vaporizing liquid thrusters, resistjets, microwave arcjets, pulsed arcjets, etc., have been proposed and are under significant development for primary and attitude control applications. In particular, the PPTs are expected to be used for microsatellites and their longterm because of the precise impulse bit controllability.[5-9)]

II. Laser assisted pulsed plasma thruster

A schematic of the rectangular laser-assisted pulsed plasma thruster (LA-PPT) is illustrated in Fig.1[14-20)] A basic idea of the system is that a bunch of laser-ablation plasma, induced through laser irradiation on a solid target, is supplied to an acceleration channel and additionally accelerated by electrical means between an anode and a cathode. When the current between the electrodes increases, the plasma can be heated and further ionized through joule heating. Thus, the electrothermal acceleration effect will be significant. With larger current exceeding more than one thousand amperes, the electromagnetic acceleration effect becomes significant. With the interaction of the current and a self-induced magnetic field, a streamwise acceleration of the plasma will be provided.[5, 21-22)] Since any solid materials can be used for the propellant in these systems, no tanks, no valves, or piping systems are required for the propulsion system. Also, various materials in any phases can be used for the propellant. Therefore, the system employing this technique can be simple and compact. As the laser-ablation plasma has a directed initial velocity of few tens of km/s, which will be further accelerated by electrical means, significantly high specific impulses can be expected.

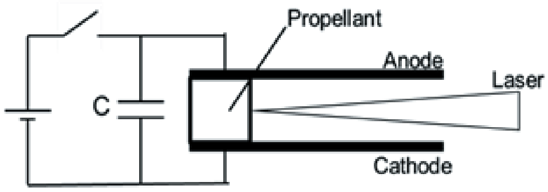

Figure 1. Schematic of a laser-assisted pulsed plasma thruster

III. Research motivation

In previous works of the LAPPTs, in which laser ablation plasma is accelerated by interaction of pulsed discharge current and self-induced magnetic field, or Lorentz force, authors have been investigating plasma acceleration characteristics and thrust performance with a combination of nanosecond laser pulse inducing laser-ablation plasma propellant from alumina ceramic and microsecond discharge pulse, and have demonstrated their high specific impulse characteristics.[20)] Fig.2 shows the typical high specific impulse characteristics of the laser-assisted pulsed plasma thruster replotted from our previous report, in which variations of specific impulse with charge energy are plotted for various acceleration channel configurations.[20)] From the figure, it can be seen in all the cases that specific impulse increased with the increase of the charge energy. Moreover, thrusters with

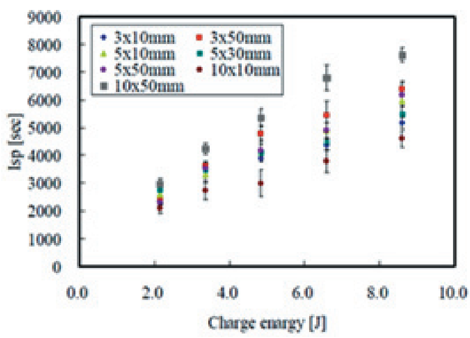

Figure 2. Variation of specific impulse with charge energy for thrusters with various electrode geometries (electrode length x electrode height).[20)]

longer channel length showed higher specific impulses. The highest specific impulse of 7,200 sec was obtained with the 10 mm x 50 mm thruster at the highest charge energy of 8.6 J.[20)] In this study, for the next step, using smaller capacitances with higher charge voltages, we could reduce the discharge pulse width from 1300 ns into 100 ns. To compare the effects of length and material of the electrodes, electrodes of 5 mm in length and those made of copper were also examined.

IV. Experiment Setup

A. Impulse bit measurement

A photo of the thruster is shown in Fig. 3, in which electrodes made of molybdenum and propellant and insulator made of alumina ceramics. Configuration of the thruster is listed in Table 1. To compare the effects of length and material of the electrodes, electrodes of 5 mm in length and those made of copper were also examined. A capacitor bank (TDK, Ultra-high Voltage Ceramic Capacitors UHV-3A, capacitance: 4 nF, total capacitance of capacitor bank: 50 nF) was utilized for short pulse operation(Fig.4.).

A short-pulse LA-PPT is placed in vacuum chamber (2.7 $\times 10^{-3}$ Pa) and ignited through laser ablation plasma induced with a focused laser pulse at a center surface of the propellant. As for the laser oscillator, an Nd:YAG laser (B.M.Industries, 5000 series , wavelength: 1,064 nm, pulse width 5 ns, maximum pulse energy: 867 mJ) was utilized. Time-resolved images were monitored with an ICCD camera (ANDOR TECHNOLOGY, minimum gate width: 2 ns).

To measure an impulse bit of a short-pulse LA-PPT, the impulse bit measurement was conducted using a cylindrical target thrust stand shown schematically in Fig.4.[23] A plasma plume, generated from the LA-PPT by an electrical discharge, comes into an entrance hole on the front plate. The bottom plate has a conical shape, and most rebounding gas particles from the bottom plate will leave radially from the target through the slits on the side of the cylinder. The main body of the cylindrical target is made of a polyvinyl chloride (PVC) plate of 0.5 mm in thickness and a pendulum arm of 300 mm in length is made of aluminum. A thruster was installed in front of the target, and impulse bit was calculated from the displacement of the pendulum. Displacement of the pendulum was measured by an inductive displacement sensor (EMIC CORP., NPA-010, resolution: 0.5 μm, range: 0 - 1.0 mm, output voltage: 0 - 1.0 V), and output signals from the sensor were monitored and recorded by an oscilloscope (Tektronix, TDS3034B, band width: 300MHz, the best sampling rate: 2.5 GS/s)

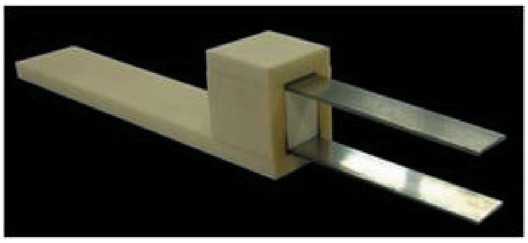

Figure 3. Schematic of photo of a rectangular LA-PPT.

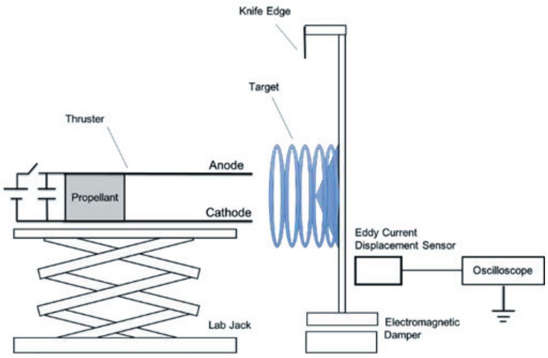

Figure 4. Schematic of an impulse bit measurement system.

Table1. Configuration of LA-PPT

Channel length: **l**	50 mm
Channel width: **w**	10 mm
Channel gap: **h**	15 mm
Electrode	Mo
Propellant	Al_2O_3
Body	Al_2O_3

B. Plasma behavior observation with ICCD camera

To observe the plasma behaviors between the rectangular electrodes of the LA-PPT, the time-resolved imaging with an ICCD camera was conducted. A schematic of experimental setup for ICCD camera observation is shown in Fig. 5.

Generating an arbitrary delay with a delay generator triggered by a Q-switch output signal of the laser, the ICCD camera was synchronized with single laser pulse and a discharge pulse, and then an image of the delay was captured at each pulse. Since the phenomena were highly reproducible, it was possible to obtain images of temporal behaviors of plasma formation and acceleration process with 2 ns resolution through changing the delay.

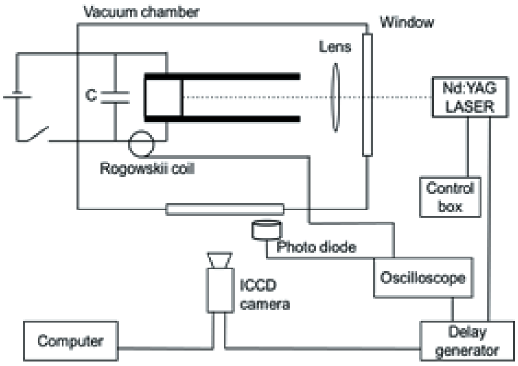

Figure 5. Schematic of experimental setup for ICCD camera.

V. Results and discussion

A. Impulse bit measurement

Some preliminary result of impulse bit of short-pulse LA-PPT (Le = 867 mJ and C = 50 nF, Mo, Al_2O_3, respectively) are shown Fig. 6, it can be seen that impulse bits increase with charge energies. The maximum impulse bits are 45 μNs at E_C = 3 J. Moreover, it cannot be seen that difference of impulse bits between material of the electrodes.

Result of impulse bits of short-pulse LA-PPT with different electrode lengths (5 mm and 10 mm) are shown Fig.7.

From the figure, it can be seen that impulse bits increase with charge energies for both electrode lengths. The maximum impulse bits at E_C = 3J are 45 μNs at l = 5 mm, 30 μNs at l = 50 mm, respectively. Moreover, for shorter electrode length case, it is shown that impulse bits are larger than longer cases.

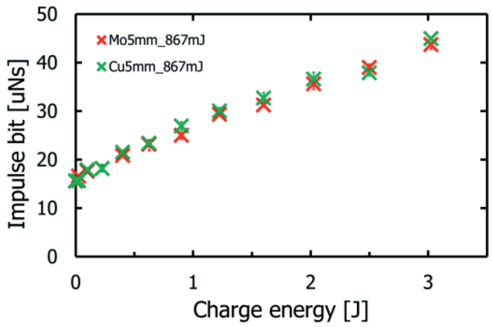

Figure 6. Impulse bit of a difference in material of the electrodes ICCD camera.

B. Plasma behavior observation with ICCD camera

ICCD images of plasma plume from short-pulse LA-PPT are shown in Fig. 8 for V_C =10 kV (E_C =1.2 J). In this figure, upper and lower white lines and a rectangular part corresponds to upper (anode) and lower (cathode) electrodes and a propellant surface, respectively. From this figure, the plasma emission can only be seen in a limited region of on and near the propellant surface. At 200 to 400 ns, strong spot emissions from the laser ablation plasma were occurring at the irradiated spot and emission along the propellant surface can also be seen. At 500 ns, similar planar emission on the surface without any spot emissions was occurring. At 650 ns, some parts of the planar emission was extending to downstream.

From the result, it was confirmed that correlations between region of plasma emissions and influence of electrodes length on impulse bits can be extracted.

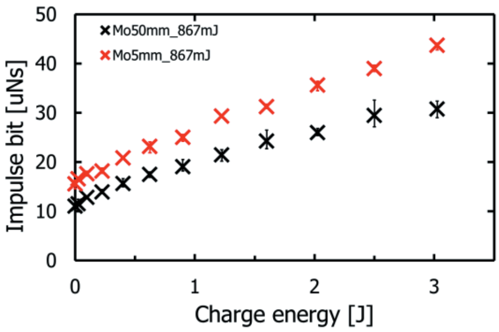

Figure 7. Impulse bit of a difference in material of the electrodes

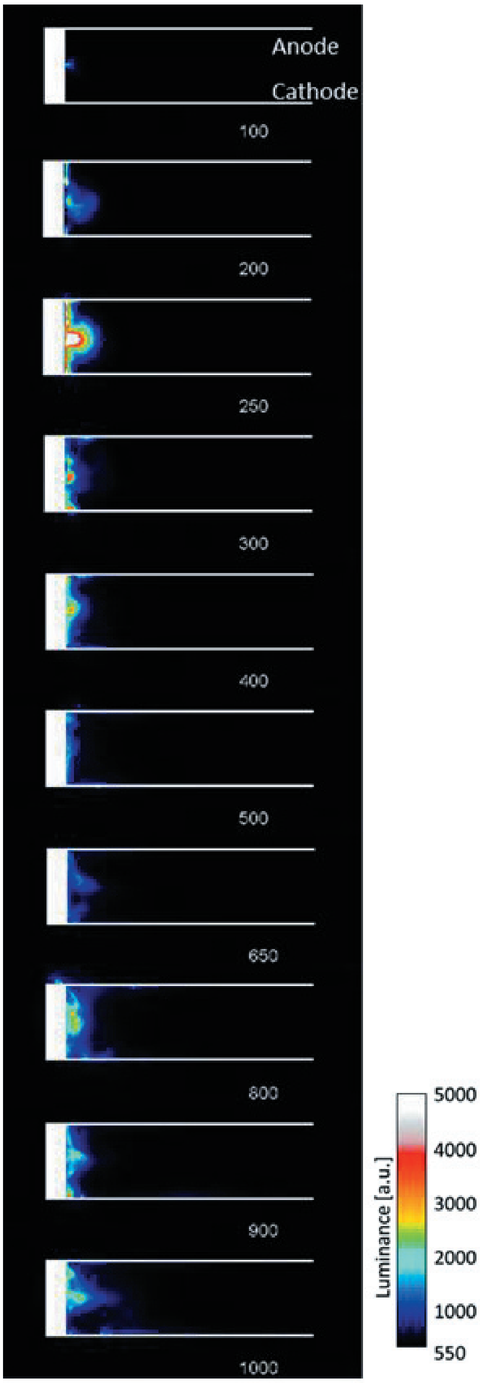

Figure 8. Time resolved images for short-pulse LA-PPT

VI. Conclusion

In this study, effects of electrode lengths and materials on thrust performance of a short-pulse rectangular laser-assisted pulsed plasma thruster (LAPPT) were investigated. Thrust performance was also examined for various cases with a target pendulum thrust stand in a vacuum chamber. To compare the effects of length and material of the electrodes, electrodes of 5 mm in length and those made of copper were also examined. Moreover, To observe the plasma behavior and the plasma acceleration process, an observation of plasma plume between the rectangular electrodes of the short-pulse laser-assisted pulsed plasma thruster with an ICCD camera was conducted.

From the results, Maximum impulse bits for charge energy of 3 J were about 40 μNs at electrodes of 5 mm in length and made of copper. It can be seen that impulse bits increase with charge energies for both electrode lengths. Moreover, for shorter electrode length case, it is shown that impulse bits are larger than longer cases. From the results of time-resolved images with the ICCD camera, the plasma emission can only be seen in a limited region of on and near the propellant surface. It was confirmed that correlations between region of plasma emissions and influence of electrodes length on impulse bits can be extracted.

References

[1]Micci, M. M., and Ketsdever, A. D. (ed.), *Micropropulsion for Small Spacecraft*, American Institute of Aeronautics and Astronautics, Astronautics and Aeronautics., 2000, 87.

[2]Burton, R. L., and Turchi, P. J., " Pulsed Plasma Thruster ", *Journal of Propulsion and Power*., Vol. 14, 1998, pp. 716–735.

[3]Gonzales, D., and Baker, R., *Micropropulsion Using a Nd:YAG Microchip Laser*, Proceedings of SPIE

[4]Myers, R. M., et al., "Small Satellite Propulsion Options," AIAA Paper, 1994, pp. 94-2997.

[5]Mueller, J., "Thruster Options for Microspacecraft: A Review and Evaluation of Existing Hardware and Emerging Technologies," AIAA Paper, 1997, 97-3058.

[6]Leifer, S., "Overview of NASA's Advanced Propulsion Concepts Activities," AIAA Paper, 1998, 98-3183.

[7]Coletti, M., and Ciaralli, S., et al., "PPT development for Nanosatellites applications: experimental results," IEPC (International Electric Propulsion Conference) Paper IEPC-2013-198.

[8]Kisaki, S., and Tahara, H., et al., "Research and Development of Electrothermal Pulsed Plasma Thruster Systems onboard Osaka Institute of Technology PROITERES Nano-Satellites," IEPC Paper -2013-97.

[9]Egami, N., and Tahara, H., et al., "R&D, Launch and Initial Operation of the Osaka Institute of Technology 1st PROITERES Nano-satellite with Electrothermal Pulsed Plasma Thrusters and Development of the 2nd Satellite," IEPC Paper 2013-100.

[10]Gabriel, S., and Rogers, S., "The Applicability of Pulsed Plasma Thrusters to Rendezvous and Docking of Cubesats," IEPC Paper, 2013, 2013-424, pp. 1-3.

[11]Pakhomov, A.V., et al., "Specific Impulse Study of Ablative Laser Propulsion," AIAA Paper, 2001, 2001-3663.

[12]Horisawa, H., and Kimura I., "Fundamental Study on Laser Plasma Accelerator for Propulsion Applications," Vacuum, 65 (2002), pp.389-396.

[13]Horisawa, H., et al., Beamed Energy Propulsion: AIP Conference Proceedings, 664 (2003), pp.423-432.

[14]Kawakami, M., et al., AIAA Paper, 2003, 2003-5028.

[15]Horisawa, H., et al., Applied Physics A., 81 (2005), pp.303-310.

[16]Horisawa, H., et al., The Review of Laser Engineering., 34 (2006), pp.435-441.

[17]Sasaki, Y., et al., IEPC Paper, 2007-56.

[18]Horisawa, H., et al, AIAA Paper, 2008, 2008-4818.

[19]Ono, T., et al, AIAA Paper, 2008, 2008-5008.

[20]Horisawa, H., "High Isp Mechanism of Rectangular Laser-Electromagnetic Hybrid Acceleration Thruster," IEPC Paper, 2011-274, pp. 7-8

[21]T.E. Markusic., "Phenomenological Model of Current Sheet Canting in Pulsed Electromagnetic Accelerators," IEPC Paper, 2003, 2003-0293, pp. 5-6

[22]Jahn, R. G., "Physics of Electric Propulsion, McGraw-Hill," 1968, pp.198-316.

[23]Yanagi, Y., Kimura, I., "New Type of Target for the Measurement of Impulse Bits of Pulsed Plasma Thrusters," J. SPACECRAFT, 19(1982), AIAA 82-4138.